This is the author's peer reviewed, accepted manuscript. However, the online version of record will be different from this version once it has been copyedited and typeset PLEASE CITE THIS ARTICLE AS DOI: 10.1063/5.0114670

Heat Generation in PZT MEMS Actuator Arrays

Charalampos Fragkiadakis, ¹ Subramanian Sivaramakrishnan, ² Thorsten Schmitz-Kempen, ¹ Peter Mardilovich, ^{1,a)} and Susan Trolier-McKinstry³

¹ aixACCT Systems GmbH, Aachen, Germany

² ARNDIT LLC, Beaverton, OR, USA

³ Materials Science and Engineering Department and Materials Research Institute, The Pennsylvania State University, University Park, PA, USA

a) Author to whom correspondence should be addressed: mardilovich@aixacct.com

Abstract

Piezoelectric microelectromechanical systems (piezoMEMS) enable dense arrays of actuators which are often driven to higher electrical fields than their bulk piezoelectric counterparts. In bulk ceramics, high field driving causes internal heating of the piezoelectric, largely due to field-induced domain wall motion. Self-heating is then tracked as a function of vibration velocity to determine the upper bound for the drive levels. However, the literature is limited concerning self-heating in thin film piezoMEMS. In this work, it is shown that self-heating in piezoMEMS transducer arrays occurs due to domain wall motion and ohmic losses. This was demonstrated via a systematic study of drive waveform dependence of self-heating in piezoMEMS arrays. In particular, the magnitude of self-heating was quantified as a function of different waveform parameters (e.g., amplitude, DC offset, and frequency). Thermal modeling of the self-heating of piezoMEMS using the measured hysteresis loss from electrical characterization as the heat source was found to be in excellent agreement with the experimental data. The self-heating model allows improved thermal design of piezoMEMS and can furthermore be utilized for functional heating, especially for device level poling.

In bulk piezoelectric actuators, the operational upper power limit is often governed by self-heating of the device. The area inside a polarization – electric field (P–E) curve corresponds to the energy lost per actuation cycle. P-E hysteresis is a result of the field-induced motion of domain walls or phase boundaries in a material with distributed pinning centers in addition to nucleation of new domains [1]. The energy dissipated during a field cycle is lost as heat, and in cases where the heat generated exceeds the heat removal by thermal conduction, convection, and radiation, the transducer temperature rises, i.e., the material self-heats in response to the drive

PLEASE CITE THIS ARTICLE AS DOI: 10.1063/5.0114670

electric field. This self-heating is exacerbated when the electrode volume/area ratio of the piezoelectric is large [2], as the radiation area is reduced.

One approach to quantify this energy loss is to measure the temperature rise as a function of the vibration velocity for the material [2-5]. The vibration velocity is the velocity of the surface as the piezoelectric is driven either off- or on-resonance. The temperature rise is then measured via infrared thermometry, or some other convenient technique. In materials where domain wall motion is substantial, unipolar P-E loops are also hysteretic; energy dissipation is high and the material self-heats at small drive fields (and hence vibration velocities). The maximum vibration velocity is often set as the vibration velocity at which the transducer temperature rises by 20°C [2].

In considering the upper limits for drive conditions for piezoMEMS actuators, it is important to note that the thermal boundary conditions differ from stack actuators or sonar arrays, etc. The surface area to volume ratio is much higher, which is useful for heat extraction (particularly for devices built on silicon-on-insulator (SOI) wafers, given the high thermal conductivity of single crystal silicon) [6]. Nonetheless, self-heating has been reported in released structures [7]. As expected, for actuation of isolated piezoMEMS devices based on lead zirconate titanate (PZT) films, the energy dissipation was larger for bipolar cycling through major hysteresis loops than for either unipolar actuation or minor hysteresis loops.

A second way in which ferroelectric films differ from bulk ceramics is the reduced extent of ferroelastic domain wall motion [8 - 12]. As a result, PZT films are "harder" than bulk PZT ceramics. Since the motion of domain walls dominates self-heating, and one population of walls is largely clamped out in films, it is not obvious that self-heating will occur to the same extent as is characteristic of PZT ceramics.

Limited data have been reported for actuator arrays driven at high frequencies. To ameliorate this lack, in this study, a test die representing an industrial thin film piezoMEMS drop-on-demand inkjet die was used to study self-heating as a function of the excitation conditions [13,14]. The die utilized 1420 sol-gel PZT-based micro-actuators arranged in four rows of 355 actuators each. The overall size of the die was 32mm×13mm×0.5mm. Measurements were performed on a single row of actuators. Electrical contacts were made to every sixth (1st, 7th, 13th etc.) actuator and the row was electrically divided into three groups, with each group containing twenty actuators. All the actuators in a group were electrically connected. Each test group (left, center, or right) could be driven independently. To perform this experiment with well-controlled thermal boundary conditions, the die was firmly attached to a polycarbonate substrate. The test die also incorporated metal resistance temperature detectors (RTDs) on both sides for temperature measurements. The RTDs were calibrated by holding the die at fixed temperatures and measuring the corresponding resistances using the 4-wire measurement method to cancel the effect of the test lead and channel path resistances. Moreover, additional resistance from thermoelectric voltages was eliminated by using offset compensation measurements [15]. For each drive condition, care was taken to ensure that the steady state temperature was reached.

PLEASE CITE THIS ARTICLE AS DOI: 10.1063/5.0114670

The temperature drift during the measurement was <0.07°C over a period of 5 minutes; the origin of the drift was human activity in the laboratory.

To measure the energy dissipated by a single actuator, P–E hysteresis measurements were performed using an aixACCT Thin Film Analyzer TFAnalyzer3000 using sinusoidal waveforms:

$$V(t) = B + A \sin(\omega t)$$
 (1)

where B is the DC offset, A is the amplitude and ω =2 π f, where f is the driving frequency. The DC offset allows a mix of bipolar and unipolar components in different proportions in the waveform. Specifically, B=0 gives a symmetric bipolar waveform (true bipolar) while |B| \geq A gives a completely unipolar (positive or negative polarity) waveform. For intermediate values of |B|<A, the waveform is bipolar but not symmetrical (offset bipolar). The self-heating was assessed over a wide range of the waveform parameters, A, B, and f.

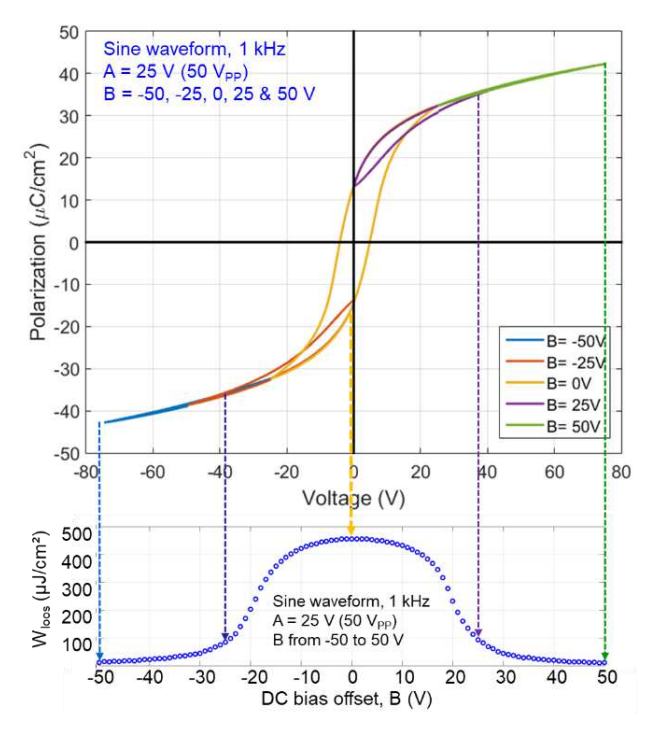


Fig. 1. Top: Polarization vs. voltage loops for sinusoidal waveform with A=25 V, f=1kHz and five different DC offset values; Bottom: hysteresis loss, W_{loss} , as a function of DC offset.

PLEASE CITE THIS ARTICLE AS DOI: 10.1063/5.0114670

Figure 1 shows the measured P–E hysteresis loops for different values of the DC offset (B) for A=25 V at 1 kHz. Typically, each loop is averaged over 200 cycles. Since the absolute value of measured polarization is arbitrary, the starting polarization for offset bipolar waveforms are shifted along the y-axis to the corresponding points for the purely bipolar waveform. This allows easy comparison between different loops. The area inside each P-E hysteresis loop gives the energy lost as heat during one cycle, Wloss, including domain switching and resistive losses, and is calculated by numerical integration.

A plot of W_{loss} as a function of the DC offset is also shown in Fig. 1. Fig. 2 shows the plots of hysteresis loss vs. DC offset, B for all values of A and f.

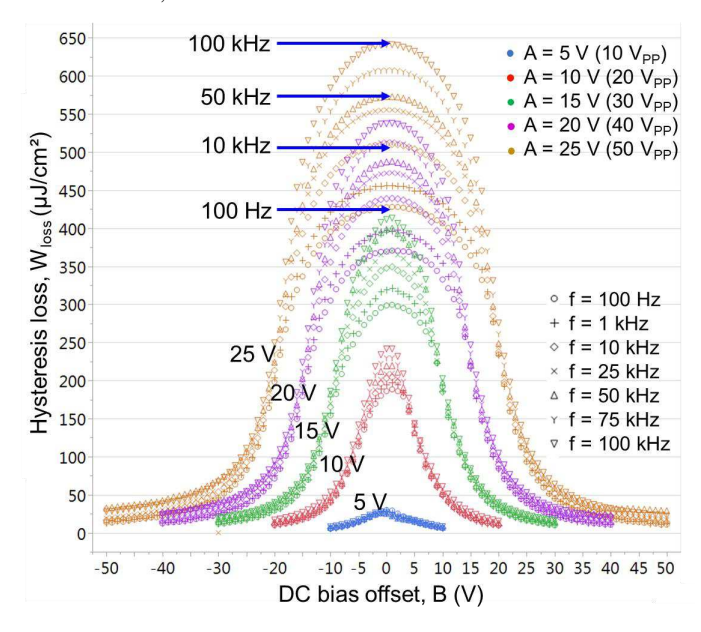


Fig. 2. Hysteresis loss for a single actuator, W_{loss} , as a function of DC offset (B) for different amplitude, A, and frequency, f.

Thermal modelling of the self-heating under steady state conditions was done via a 3D Finite Element Model (FEM) of the die geometry in COMSOL as shown in Fig. 3. The materials properties utilized are listed in Table I.

Table I. Materials in the modelled stack, their thickness, density and thermal properties.

eset.

(Ď
5	\geq
4	\rightarrow
7	2
2	2
-	5
6	
	_
7) }
5	Σ.
2	2
5	3
_	_
2	D.
	Б
_	2
0	
0	
_	-
-	=
0	Ď
2	2
- 6	5
2	-
- 6	5
Š	0
ò	<u></u>
- 5	5
C	0
+	_
8	
5	\supset
4	
÷	Ξ
Š	Ď
2	Ī)
#	Ĕ
Ë	5
	15
2	5
Ξ	
.2	>
_	_
3	2
9	Ś
6	5
2	_
4	5
0	_
2	5
- 6	<u></u>
5	_
2	N N
5	_
VOV	_
ino vor	_
nling you	_
online yer	_
nling you	_
o online ver	_
r the online yer	, IIIO OIIIIIO VOI:
ho online ver	ו, נווס סוווווס עמוי
yor the online you	evel, tile Olillie vel
r the online yer	wevel, the offine ver
owever the online yer	evel, tile Olillie vel
yor the online you	wevel, the offine ver
# However the online yer	. HOWEVEL, LITE OFFICE VELS
nt Howaver the opline ver	wevel, the offine ver
crint Howaver the online ver	. HOWEVEL, LITE OFFICE VELS
# However the online yer	solpt. However, the offine ver
neorint Howaver the online ver	olpt. Howevel, the olime ver
anisorint Howayar the poline yar	Haseript. However, the offille vers
anisorint Howayar the poline yar	solpt. However, the offine ver
niegript Howaver the online ver	Haseript. However, the offille vers
anisorint Howayar the poline yar	Haseript. However, the offille vers
ted manuscript Howayer the online yer	ted mandacript. However, the offine vers
and managerint Howards the paline yer	apteu manuscript. However, the offine vers
cented manuscript However the online ver	cepted manascript. However, the offilie vers
contact manuscript However the online very	depted mandodipt. However, the diffile vers
maning Mountaint Howayar the poline yer	, accepted manuscript. However, the offine vers
you adjac ad the Howard the called you	i, accepted manascript. However, the offille vers
you eall ac eat * You would * Animan I had a so the your	, accepted manuscript. However, the offine vers
yev earlier alwayer the contract	waa, accaptaa mamasanpu mowaya, ma omma yan
yev earling oth Towayer Howard Laws	iewaa, accaptaa mamaanpi, mowavat, ma omma vata
you earlier a However the contract and a second according to the contract and a second according to the contract and a second a s	iewaa, accaptaa mamaanpi, mowavat, ma omma vata
reviewed secretary manuscript However the colline way	iewaa, accaptaa mamaanpi, mowavat, ma omma vata
reviewed accepted manager to Howaver the collection	Heviewed, accepted manuscript. However, the offine vers
ar reviewed eccepted manuscript However the online very	a Taviawaa, accaptaa mamasaipt. Howayai, ma oiima yais
reviewed accepted manager to Howaver the collection	del Taviawau, acceptad manuscript, Mowava, ind Olima vers
ania ad assertion Howard management Howard the variation	poor reviewed, accepted manuscript. However, the offilie vers
on a property of the second se	ו א שלמו ולאומיעילע, מכנסטונים וומושאטוטו. ווטיעלעלו, ווס טוווווס עלו
ar's near reviewed accounted manuscript Howaver the puline yes	ol a pagi laviawau, accaptau mamasciipt. Howavai, ma oiiiina vais
on a property of the second se	illoi a paar raviawaa, accaptaa mamaanpi. Howavar, illa oillilla var.
Thor's poor reviewed accompany mannessing However the paline yer	מוווסן פ מספר וסעופעיסע, מככסמוסע ווומוועפטומני ווסעיסעו, וווס טוווווס עקו
author's poor reviewed posested measured However the palies yes	autilot a pedi teviewed, accepted illatidactipit, flowever, tile offille ver
author's poor reviewed posested measured However the palies yes	ia autiloi o pagi laviawau, accaptau illalidodipt. Llowavat, tila Oliilla vat.
the author's peer reviewed perented montes However the peline yer	illa autillo o pagi laviawau, accaptau mamaocipti, mowavai, ma omina vai.
the author's peer reviewed perented montes However the peline yer	illa autillo o pagi laviawau, accaptau mamaocipti, mowavai, ma omina vai.
is the author's pact reviewed eccepted measurerist. However the caline ver	is the author of peer reviewed, accepted manuscript. However, the office ver
the author's peer reviewed perented montes However the peline yer	is the author of peer reviewed, accepted manuscript. However, the office ver

PLEASE CITE THIS ARTICLE AS DOI: 10.1063/5.0114670

Material	Thickness	Density	Thermal Conductivity	Specific heat capacity
	(µm)	(K/m^3)	$(W/(m \cdot K))$	$(J/(kg \cdot K))$
PZT	2	7750	1.4	430
SiO ₂	1.5	2200	1.4	730
Si (top)	400	2329	130	700
Si (chamber)	70	2329	130	700
Si (nozzle plate)	50	2329	130	700
Polycarbonate	1200	1200	0.2	1250

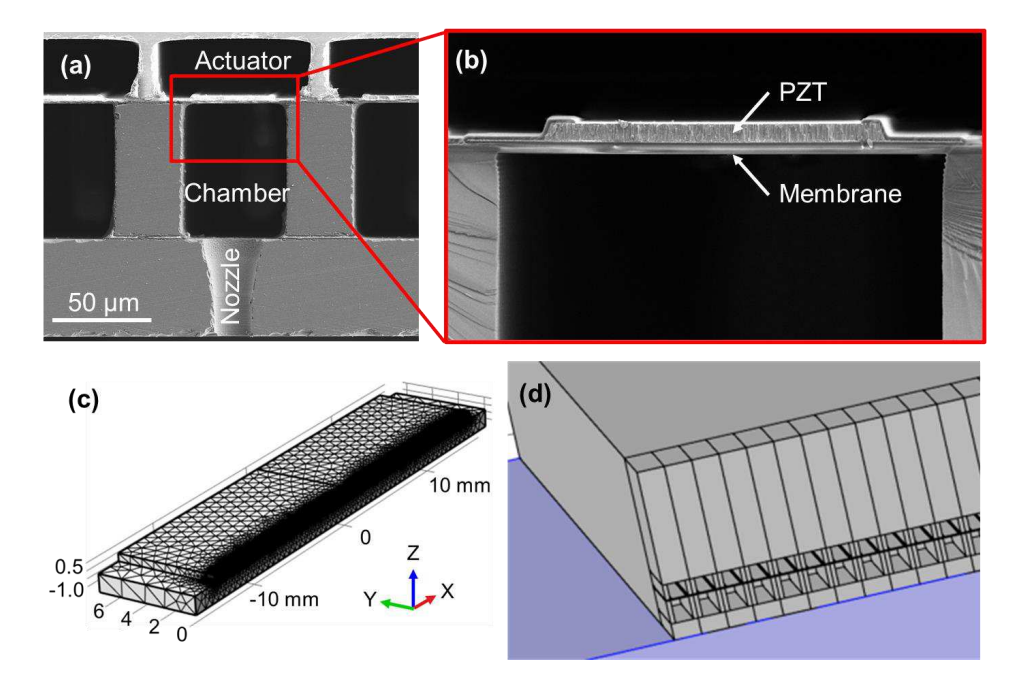


Fig. 3. SEM cross-section of a die (a) and an individual actuator (b). Full geometry (c), dimensions in mm, and a zoom-in view of the individual actuators (d) of the FEM model (the front face is a cut-plane across the middle of a row of actuators).

In this model, W_{loss} data from Fig. 2 was used as the heat source. The modeled heat dissipation mechanisms are convection from the ambient-exposed surfaces of the die and conduction through the polycarbonate substrate. The ambient as well as the bottom surface of the substrate

PLEASE CITE THIS ARTICLE AS DOI: 10.1063/5.0114670

were assumed to be held at 20°C. While the overall die size is 32×13×0.5 mm, the individual actuators are small (~55 µm×1 mm×~5 µm). Accurate actuator dimensions and locations are needed to model the source of heat correctly. At the same time, it is also important to maintain accurate the overall dimensions of the die to correctly model the heat loss mechanisms. This presents a challenging problem in terms of the overall grid elements of the model. In order to reduce the complexity of the model, only the actuated row included all the actuators with their dimensions while treating the three unactuated rows as silicon. The model uses a combination of structured (prism) and unstructured (tetrahedral) elements with a quadratic discretization scheme. The mesh density was increased until the results were consistent and stable. The final model used $\sim 6 \times 10^5$ mesh nodes. Further doubling of the mesh density did not change the results.

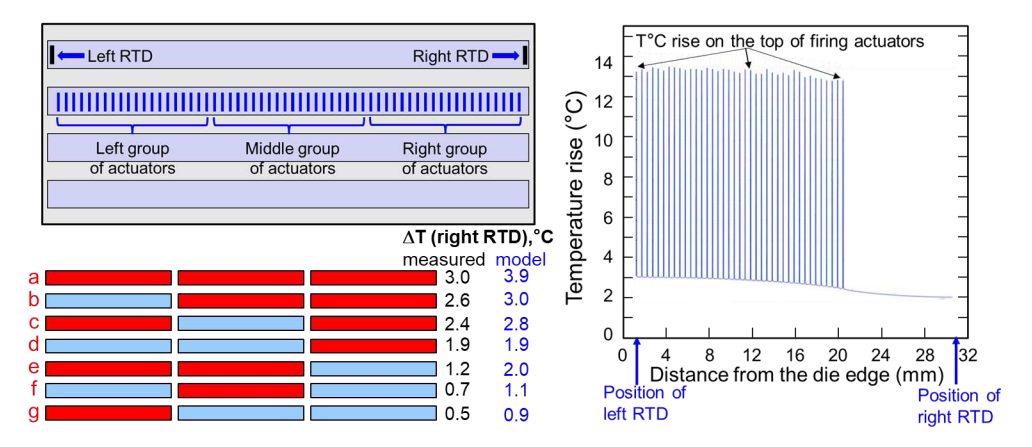
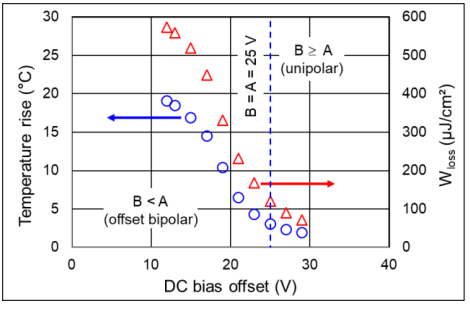


Fig. 4. Top-left: schematic of the die, showing four rows; measurements were performed on a single row of actuators. Bottom-left: seven combinations: "a" to "g", of fired actuators (those shaded red are fired and those in blue are not) and the temperature rise measured by the RTD and modelled at the right side of the die. Right: steady state temperature rise distribution inside the die from a 3-D FEM when two groups of actuators are fired (option "e") using A=25 V, B=25 V and f=100 kHz; each peak corresponds to a local temperature rise on the top of a fired actuator.

Figure 4 shows a schematic of the die with the relative location of the RTDs, three groups of electrically connected actuators (20 actuators each, total 60) and a representation of seven different combinations of groups of actuators fired. A sinusoidal waveform with A=25 V, B=25 V and f=100 kHz was used in this experiment. Fig. 4 also includes the temperature rise measured on the right side of the die and the modeled temperature rise. The agreement between the measured and the modeled temperature rise is good. The small difference between the two is attributed to discrepancies in the actual thermal properties of the materials (especially, the polycarbonate substrate) and the values assumed in the model. The temperature distribution

PLEASE CITE THIS ARTICLE AS DOI: 10.1063/5.0114670

across all 355 actuators in a row as obtained from FEM is also shown in Fig. 4. The local temperature of the fired actuators is about 10° C higher than the temperature at the ends of the die (Fig. 4 right).



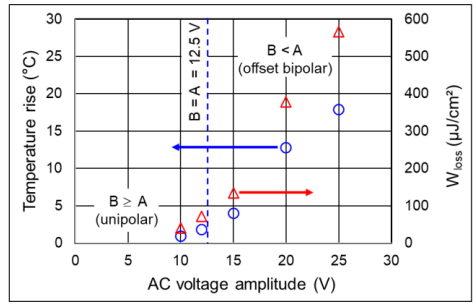


Fig. 5. Temperature rise when 60 actuators are fired and single actuator hysteresis loss, W_{loss} , as a function of DC bias offset B, with A=25 V (left) and as a function of AC amplitude A, with B=12.5 V (right) for f=100 kHz.

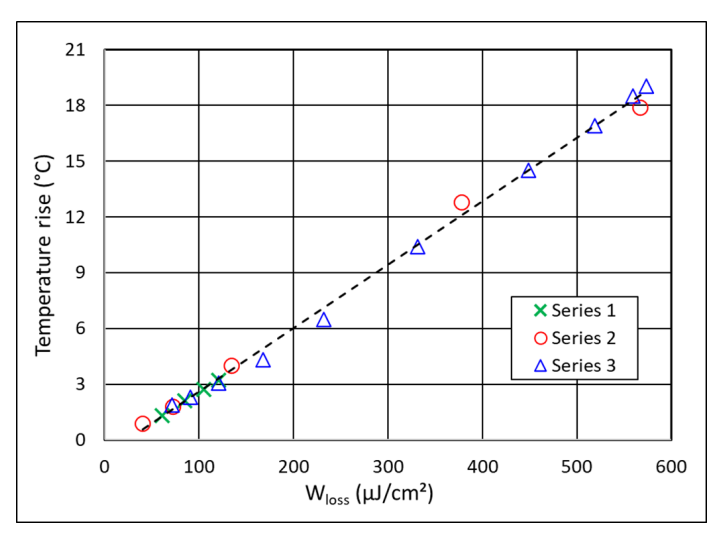


Fig. 6. Temperature rise when 60 actuators are fired as a function of single actuator hysteresis loss, W_{loss} for various A and B at a frequency of 100 kHz. Series 1: A=B, A/B sweep; Series 2:

PLEASE CITE THIS ARTICLE AS DOI: 10.1063/5.0114670

B=12.5 V, A sweep; Series 3: A=25 V, B sweep. The slew rate in series 1 and 2 varies from 5.6 to 14 V/µs; for Series 3, the slew rate is fixed at 14 V/µs.

Figure 5 plots the temperature rise when all 60 actuators are fired and the single actuator W_{loss} as a function of DC bias offset (B) and the AC amplitude (A) for a fixed frequency of 100 kHz. For a "B sweep," A was constant at 25 V and B was varied from 12 to 29 V. For the "A sweep," the DC bias offset B was 12.5 V and A was varied from 10 to 25 V. In both cases, the temperature rise scales with W_{loss}. Fig. 6 shows the measured temperature rise as a function of hysteresis loss-for various combinations of A and B at a fixed frequency of 100 kHz. The linearity of the plot implies that the temperature rise is directly proportional to W_{loss}. Furthermore, varying the slew rate from 5.6 to 14 V/µs did not affect this linear relation.

There are several key points to recognize from these data. First, this approach to measuring the temperature is both quantitative and free from the limitations arising from the field-induced flexure of piezoMEMS that complicates conventional measurements by IR thermometry or thermoreflectance [7]. Second, the temperature changes, even under unipolar excitation can be large for arrays of piezoMEMS actuators (especially noting that in these measurements only 60 out of 1420 actuators were driven). Third, the maximum W_{loss} in Fig. 2 corresponds to the purely bipolar waveforms; as the unipolar component of the waveform increases, W_{loss} also decreases due to increased stabilization of the domain state. The energy loss is also a function of waveform amplitude, as expected [16].

Fourth, this paper addresses only high field dielectric loss as measured by the P-E hysteresis loops. The elastic and piezoelectric losses [2, 4, 17, 18] are not included, save that the fundamental mechanisms associated with motion of domain walls are also captured in the dielectric losses. It is noted that the operating conditions considered in this study are far from the electro-mechanical resonance frequency of the actuator, which is ~2.75 MHz. Thus, the contribution to heat generation from the mechanical and piezoelectric losses is believed to be smaller than that due to the dielectric loss. In addition, the motion of non-180° domain walls is significantly reduced in films [8-12], which will also reduce the elastic and piezoelectric losses.

Fifth, if the electrode resistance is known, it is possible to quantitatively separate the contributions to self-heating from Ohmic losses in the electrodes from those associated with domain wall motion in the ferroelectric as a function of frequency. For a quantitative estimation of Ohmic loss, the root mean square current, I_{RMS}, associated with each of the P-E loops was measured. The Ohmic loss in the electrodes is given by:

$$W_E = I_{RMS}^2 R T_p \tag{2}$$

where R is the total DC resistance of the electrodes (130 ohms) of a single actuator, including top, bottom electrodes and connecting metal traces and $T_p=2\pi/\omega$ is the cycle period of the loop. The ohmic loss varies linearly with frequency since I_{RMS} varies as j ω C and T_p varies as 1/ ω .

This is the author's peer reviewed, accepted manuscript. However, the online version of record will be different from this version once it has been copyedited and typeset PLEASE CITE THIS ARTICLE AS DOI: 10.1063/5.0114670

This Ohmic loss can be subtracted from the measured W_{loss} to calculate the energy loss associated with the domain wall motion. Fig. 7 shows plots of the frequency dependence of Ohmic loss and the energy loss due to the domain wall motion for unipolar, bipolar and DC biased unipolar waveforms on a single actuator.

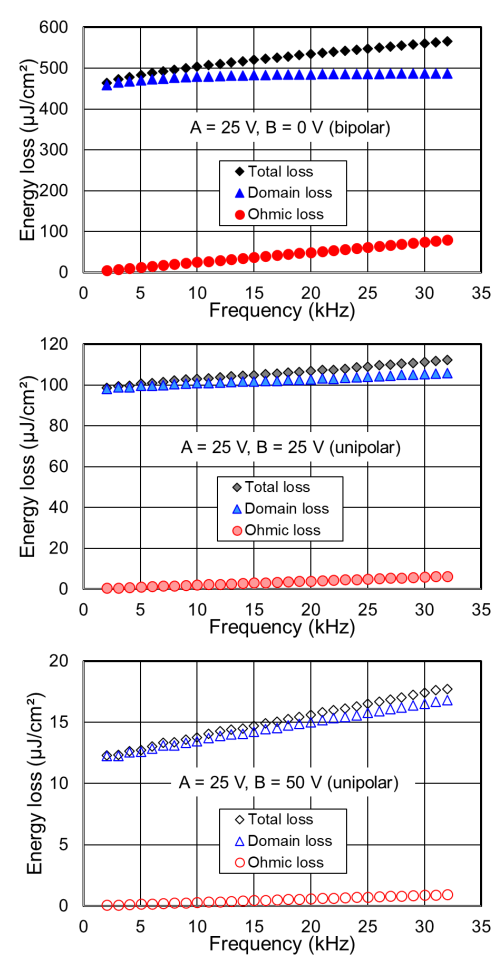


Fig. 7. Total hysteresis loss, Ohmic loss in the electrodes and the energy loss due to the domain wall motion for a single actuator as a function of frequency for bipolar (A=25 V and B=0 V), unipolar (A=B=25 V), and DC biased unipolar (A=25 V and B=50 V) sinusoidal waveforms.

This is the author's peer reviewed, accepted manuscript. However, the online version of record will be different from this version once it has been copyedited and typeset. PLEASE CITE THIS ARTICLE AS DOI: 10.1063/5.0114670

Several points are noteworthy from Fig. 7. For the unipolar case, the resistive contribution is comparatively small (\sim 6% of the total W_{loss}) even at 32 kHz. Furthermore, the calculated energy loss due to the domain wall motion is weakly dependent on frequency. On the other hand, for the bipolar waveform, the Ohmic contribution accounts for up to 14% of the energy loss at 32 kHz. This is due to the larger switching current associated with bipolar waveforms. In this case, the calculated energy loss due to the domain wall motion increases slightly up to 20 kHz. Experimentally, any decrease at higher frequencies would be due to a combination of the bandwidth of the amplifier and the voltage drop across the resistors, such that the actuator sees a waveform distorted from a pure sinusoidal shape. Thus, even in cases where the instrumentation is not power limited resistive thin film electrodes may preclude the ability to reach the desired voltage at high frequencies. This suggests that particularly for piezoMEMS with large permittivities and polarizations, design of the electrode to minimize resistance-capacitance (RC) time constant artifacts is essential. Electrode losses can often be neglected in modeling of bulk actuators [19], and are also ignored in some models of hysteresis loss in thin film ferroelectrics [20].

The linear relationship between the temperature rise and W_{loss} can be understood using a simple model that equates the total heat generation rate to the rate of heat loss by convection from all ambient-exposed surfaces and by conduction through the polycarbonate substrate, under steady state conditions. Using this model, the temperature rise can be expressed as

$$\delta T = \frac{G}{(hA_{conv} + \sigma_{sub}A_{cond}/t_{sub})} \tag{3}$$

where G is the heat generation rate given by the hysteresis loop area multiplied by frequency (thus, $G=W_{loss}$, f), h is the heat transfer coefficient for convection, A_{conv} is the total surface area for the heat loss by convection, σ_{sub} is the thermal conductivity of the substrate, A_{cond} is the die bottom surface area in contact with the substrate and t_{sub} is the thickness of the substrate. In this model, all the exposed die surfaces are assumed to be at the same measured temperature. This assumption is reasonably good since the conductivity of Si is much larger than that of the substrate (polycarbonate, 6" diameter, 1.2 mm thick). Eq. 3 is a mathematical model of the line in Fig. 6, where the slope of the line is the inverse of the denominator in eq. 3. Using the parameters given in Table II, the predicted slope of the line is 0.0038 °C/(μ J/cm²) which agrees well with the actual value of the slope of the line $(0.0034 \ \mu$ J/cm²) in Fig. 6.

Table II. Values of the parameters in eq. 3

Parameter	Value	Units
Heat transfer coefficient (h)	10	W/(m ² ⋅K)
Surface area for convection (A _{conv})	0.00064	m^2
Substrate thermal conductivity (σ_{sub})	0.2	W/(m⋅K)
Substrate area for conduction (A _{cond})	0.00042	m^2
Substrate thickness (t _{sub})	0.0012	m

PLEASE CITE THIS ARTICLE AS DOI: 10.1063/5.0114670

Of the two main mechanisms of heat dissipation considered, modelling shows that convection contributes only ~8% of the total heat dissipation. The majority of the heat removal from the die takes place by conduction through the substrate, even in the case of a moderate heat conductor like polyimide. Thus, in applications of MEMS array actuators, a good thermal conductor should be utilized for the heat sink to keep the die cool. On the other hand, self-heating can be used advantageously for poling; in this case, either a thermally insulating substrate or a free-standing die could be used. The measured die temperatures are consistent with the estimated temperatures from FEM as well as the simplified model given in eq. 3. Hence, the simplified model with known geometrical and thermal properties of the die and the substrate can be used to estimate the rise in die temperatures for different waveforms. It is significant that the temperature rise of the entire die can be as high as 20°C when only 4.2% of the actuators are fired. In the case when all 1420 actuators are fired with a unipolar waveform, the temperature rise can exceed 100°C and can be used for PZT poling [21].

In conclusion, detailed measurements of P-E hysteresis loss as a function of AC amplitude, DC bias, and frequency were used to investigate self-heating in piezoelectric MEMS actuator arrays. This methodology allows precise modeling, distinction of loss mechanisms, and prediction of temperature rise in devices as a function of the operating conditions. Good agreement is seen for temperature rise for different operating conditions in comparing RTD measurements and FEM. It was found that, unlike the case for most PZT ceramics, Ohmic heating from the electrodes is a significant fraction of the total self-heating. For high frequency piezoMEMS operation, design of the electrodes is critical to prevent excessive self-heating of the devices. Detailed understanding of the loss mechanisms allows optimized conditions for both device operation and intentional self-heating, e.g. for poling.

References

- 1. I. Mayergoyz, The Science of Hysteresis, Volume III, Academic Press, Oxford, 2006
- 2. K. Uchino, J. H, Zheng, Y. Gao, S. Ural, S.-H. Park, N. Bhattacharya, and S. Hirose, "Loss Mechanisms and High-power Piezoelectric Components," in Handbook of Advanced Dielectric, Piezoelectric, and Ferroelectric Materials, ed, Zuo-Guang Ye, Woodhead Publishing Limited, Cambridge, England (2008)
- 3. S. Takahashi, M. Yamamoto, and Y. Sasaki, "Nonlinear Piezoelectric Effect in Ferroelectric Ceramics," Jpn. J. Appl. Phys. Part 1, 37 (9B) 5292-5296 (1998).
- 4. K. Uchino and S. Hirose, "Loss Mechanisms in Piezoelectrics: How to Measure Different Losses Separately," IEEE Trans. Ultrason. Ferro. Freq. Control 48 (1) 307-321 (2001).
- 5. M. Hagiwara, S. Takahashi, T. Hoshina, H. Takeda, and T. Tsurumi, "Analysis of Nonlinear Transient Responses of Piezoelectric Resonators," IEEE Trans. Ultrason. Ferroelec. Freq. Cont. 58 (9) 1721-1729 (2011).

This is the author's peer reviewed, accepted manuscript. However, the online version of record will be different from this version once it has been copyedited and typeset PLEASE CITE THIS ARTICLE AS DOI: 10.1063/5.0114670

- 6. Y.S. Touloukian, "Thermal Conductivity: Nonmetallic Solids" (Thermophysical Properties of Matter, Volume 2) Springer, 1971.
- 7. J.S. Lundh, W. Zhu, S. Won Ko, C. Fragkiadakis, P. Mardilovich, S. Trolier-McKinstry and S. Choi, "Local Measurements of Domain Wall-induced Self-heating in Released PbZr_{0.52}Ti_{0.48}O₃ Films," J. Appl. Phys. 128, 214102 (2020); https://doi.org/10.1063/5.0029582).
- 8. N. Bassiri Gharb, I. Fujii, E. Hong, S. Trolier-McKinstry, D. V. Taylor, and D. Damjanovic, "Domain Wall Contributions to the Properties of Piezoelectric Thin Films," J. Electroceramics 19, 47–65 (2007).
- 9. F. Xu, S. Trolier-McKinstry, W. Ren, B. M. Xu, Z. L. Xie, and K. L. Hemker, "Domain Wall Motion and its Contribution to the Dielectric and Piezoelectric Properties of Lead Zirconate Titanate Films," J. Appl. Phys. 89 (2) 1336-1348 (2001).
- 10. R. Keech, C. Morandi, M. Wallace, G. Esteves, L. Denis, J. Guerrier, R.L. Johnson-Wilke, C.M. Fancher, J.L. Jones, and S. Trolier-McKinstry, "Thickness Dependent Domain Reorientation in 70/30 Lead Magnesium Niobate Lead Titanate Thin Films," J. Am. Ceram. Soc. 100 (9) 3961-3972 (2017).
- 11. M. Wallace, R. L. Johnson-Wilke, G. Esteves, C. M. Fancher, R. H. T. Wilke, J. L. Jones, and S. Trolier-McKinstry, "In situ Measurement of Increased Ferroelectric/Ferroelastic Domain Wall Motion in Declamped Tetragonal Lead Zirconate Titanate Thin Films," J. Appl. Phys. 117 054103 (2015).
- 12. R. L. Johnson-Wilke, R. H. T. Wilke, M. Wallace, A. Rajashekhar, G. Esteves, Z. Merritt, J. L. Jones, and S. Trolier-McKinstry, "Ferroelectric/Ferroelastic Domain Wall Motion in Dense and Porous Tetragonal Lead Zirconate Titanate Films," IEEE Trans. Ultrason. Ferroelec. Freq. Control 62 (1) 46-55 (2015).
- 13. P. Mardilovich, C. Fragkiadakis, S. Won Ko, and S. Sivaramakrishnan, "A new standard for thin film actuator with sol-gel PZT," Proc. of Printing for Fabrication (NIP 2017), Denver, CO, November 2017, 2761744, p.133-135.
- 14. R. Borrell, "The adoption of Thin Film PZT Si-MEMS inkjet printheads in industrial applications: the Xaar 5601", Digital Printing Conference, Barcelona, September 2017.
- 15. Low Level Measurements Handbook, 7th ed., Keithley, 2013.
- 16. R. Yimnirun, S. Wongsainmai, Y. Laosiritaworn, and S. Ananta, "Uniaxial Stress Dependence and Scaling Behavior of Dynamic Hysteresis Responses in Soft PZT Ceramics," Proc. 2006 15th IEEE International Symposium on Applications of Ferroelectrics, p. 37-41 (2007).

PLEASE CITE THIS ARTICLE AS DOI: 10.1063/5.0114670

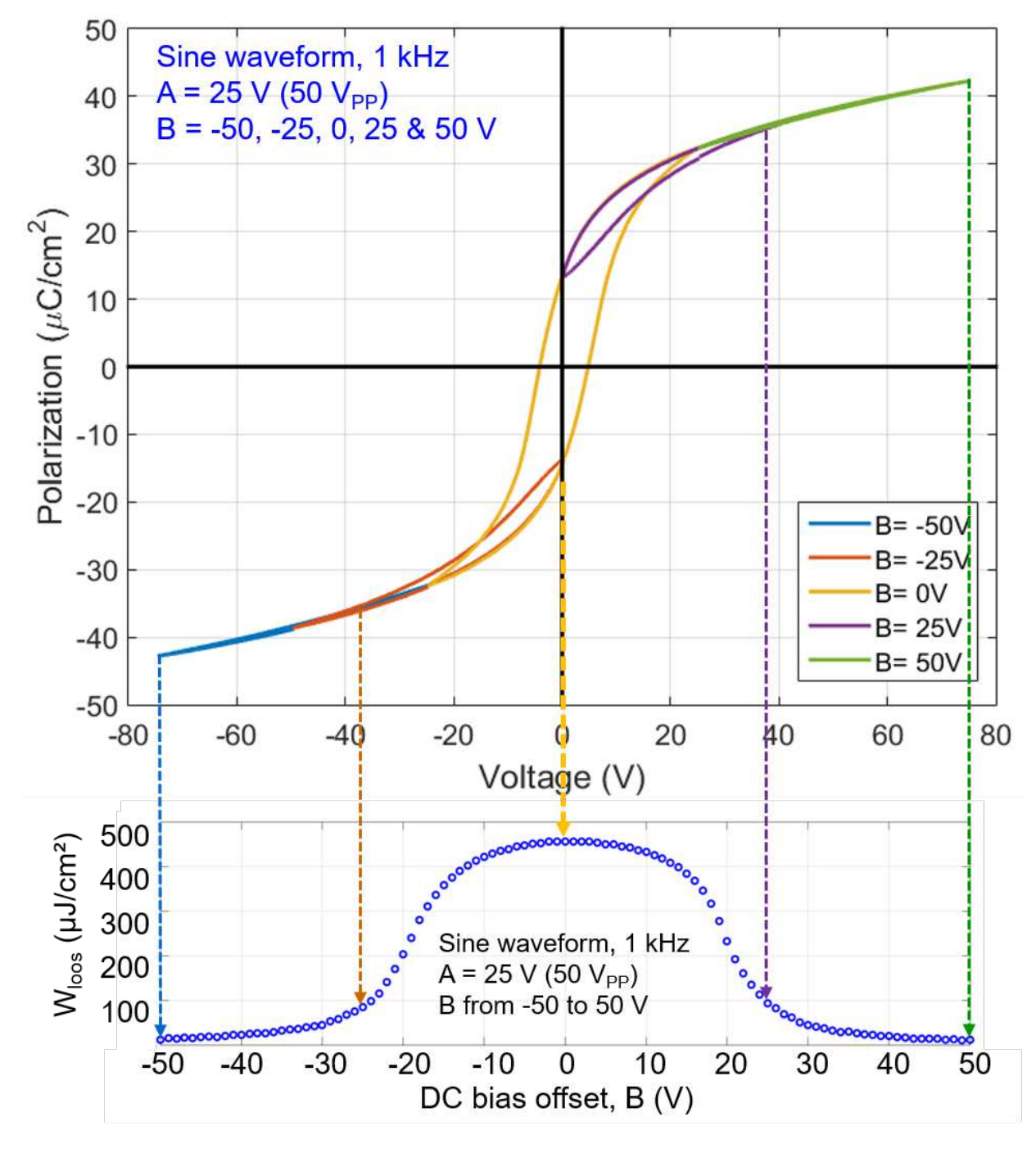
- 17. K. Uchino, Y. Zhuang, and S. Ural, "Loss Determination Methodology for a Piezoelectric Ceramics: New Phenomenological Theory and Experimental Proposals," J. Adv. Dielectrics 1(1) 17-31 (2011).
- 18. W. Shi, H. N. Shekhani, H. Zhap, J.Ma, Y. Yao, and K. Uchino, "Losses in Piezoelectric Derived from a New Equivalent Circuit," J. Electroceramics 35, 1-10 (2015).
- 19. L. M. Weiland and C. S. Lynch, Thermo-electro-mechanical Behavior of Ferreoelctric Materials Part II: Introduction of Rate and Self-heating Effects," J. Intell. Mat. Syst. Struct. 14 605-621 (2003).
- 20. J-M. Liu, H. L. Chan, and C. L. Choy, "Scaling Behavior of Dynamic Hysteresis in Multidomain Spin Systems," Mat. Lett. 52, 213-219 (2002).
- 21. C. Fragkiadakis, P. Mardilovich and S. Trolier-McKinstry, "A method of poling piezoelectric elements of an actuator", GB 25770707 B, 2021.

Acknowledgements

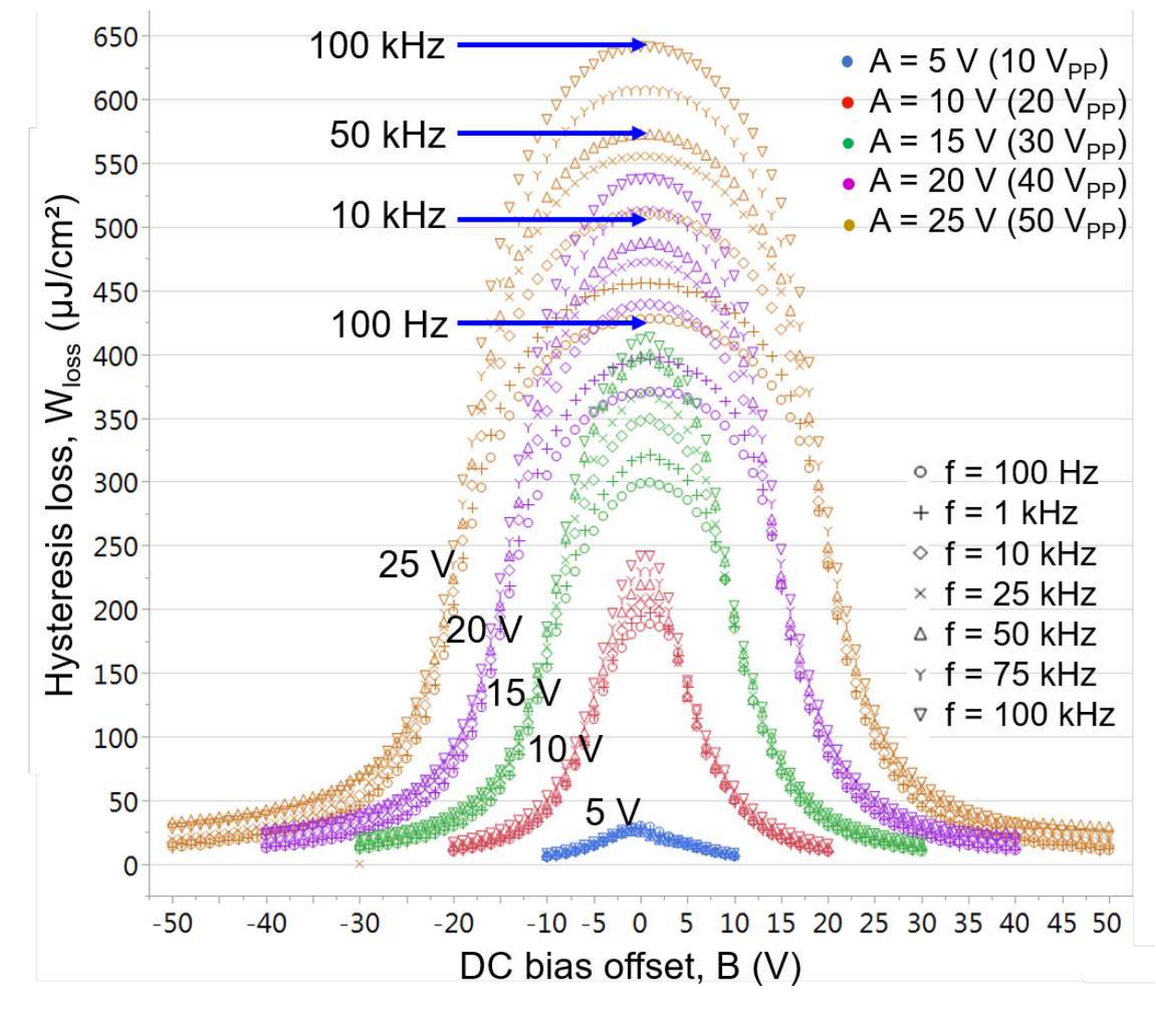
Authors wish to thank XAAR plc for allowing to use their test dies in this study. STM also gratefully acknowledges support from the National Science Foundation (NSF) through grant DMR-2025439 and the Center for Dielectrics and Piezoelectrics, North Carolina State University (CDP) under Grant Nos. IIP-1841453 and IIP-1841466.

This is the author's peer reviewed, accepted manuscript. However, the online version of record will be different from this version once it has been copyedited and typeset.

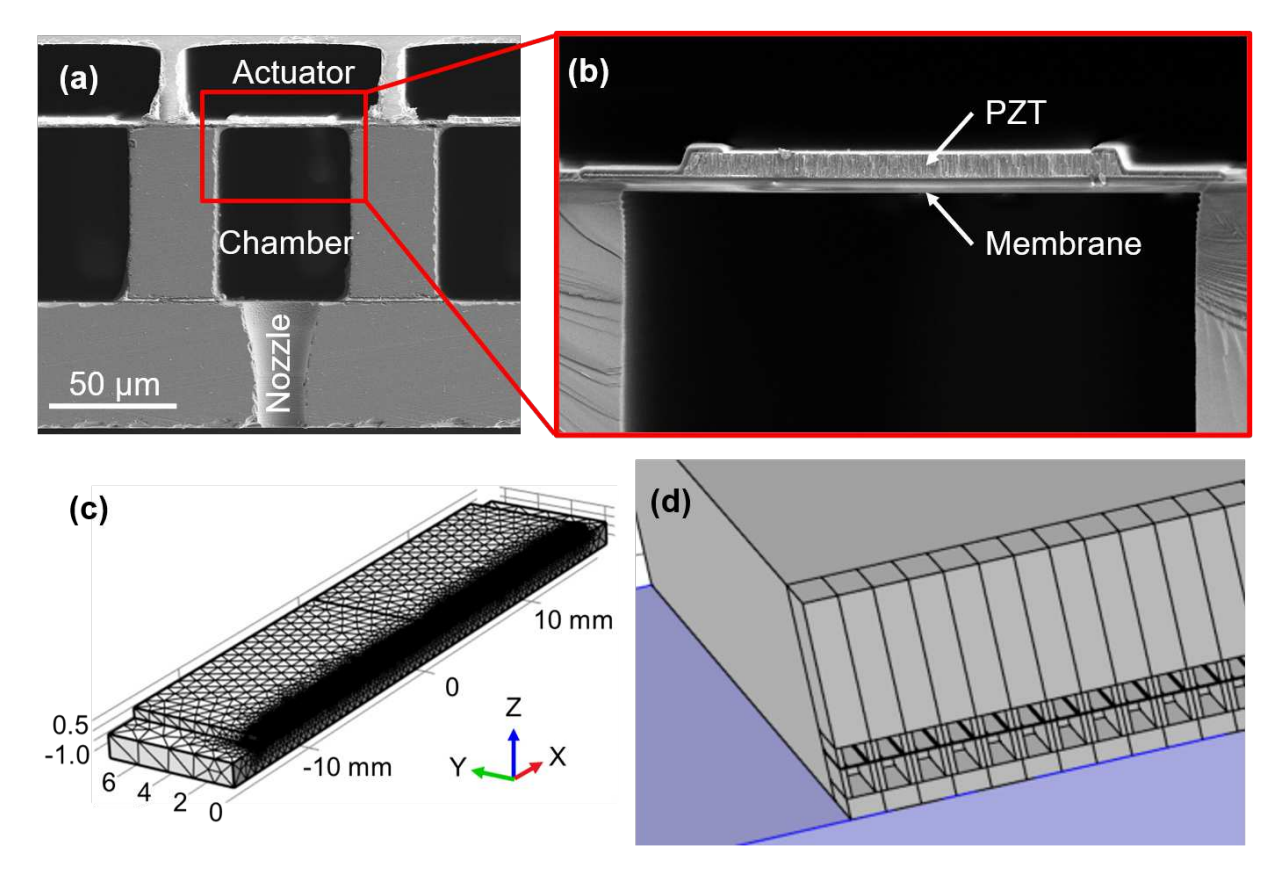




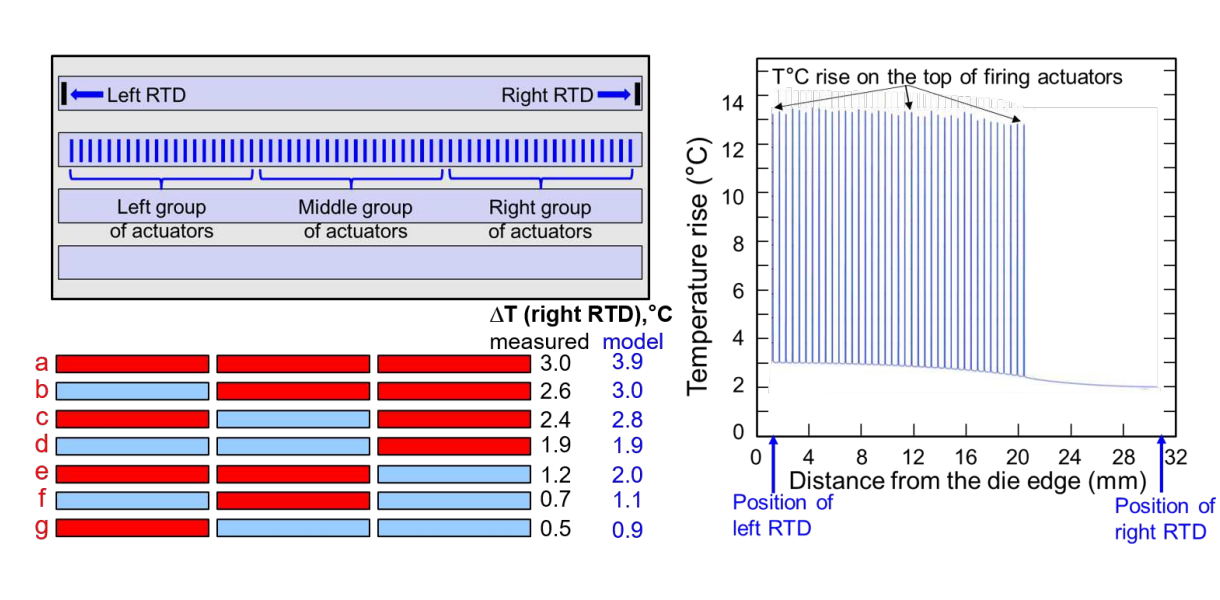
This is the author's peer reviewed, accepted manuscript. However, the online version of record will be different from this version once it has been copyedited and typeset



This is the author's peer reviewed, accepted manuscript. However, the online version of record will be different from this version once it has been copyedited and typeset.

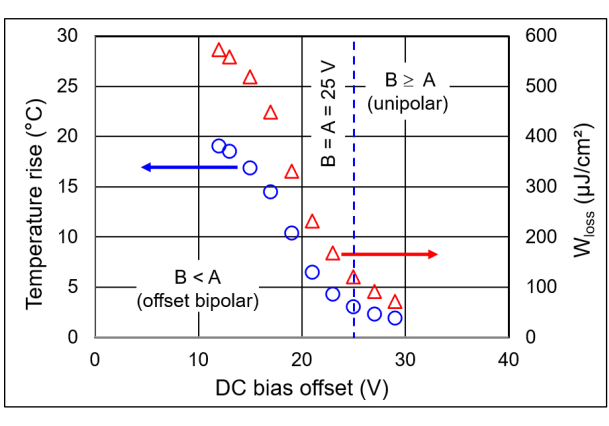


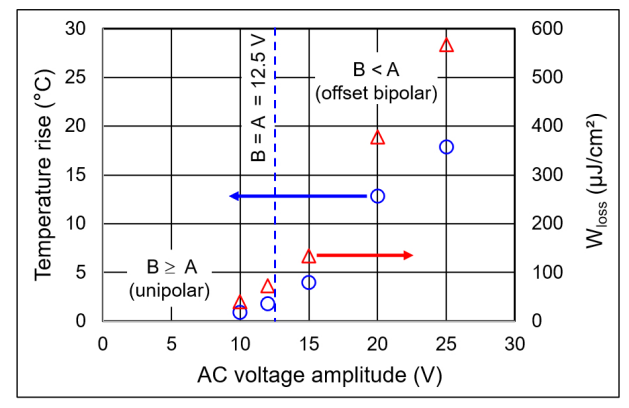














This is the author's peer reviewed, accepted manuscript. However, the online version of record will be different from this version once it has been copyedited and typeset.

